Chapter

# Production of Solketal Using Acid Zeolites as Catalysts

*Vinicius Rossa, Gisel Chenard Díaz, Germildo Juvenal Muchave, Donato Alexandre Gomes Aranda and Sibele Berenice Castellã Pergher*

## Abstract

Commercial solketal is known as Augeo™ SL 191 and is produced by Rhodia (a member of the Solvay Group), which stands out as a slow evaporation solvent derived from glycerin which is considered a renewable source. It has low toxicity to human health and the environment. It is a good solvent for resins and polymers, replacing solvents derived from petroleum, and can be used as an additive of (bio) fuels. This work aimed to study acidy zeolites (H-BEA, H-MOR, H-MFI, and H-FER) as new heterogeneous catalysts of solketal production, through the ketalization reaction of glycerol with acetone. The catalytic activity showed H-BEA > H-MOR = H-MFI > H-FER after 180 min, in kinetics study. The major conversion was 85% for H-BEA. It was also verified that all the catalysts can be reused four times without washing or pretreatment among reactions in batch reactor. The solketal produced in this work was characterized by comparing it with its commercial standard, obtaining very similar characteristics.

**Keywords:** glycerol, zeolites, ketalization, solketal, catalysis

## 1. Introduction

The main goal of the Paris Treaty is to reduce the emission of harmful gases to the planet ($CO_x$, $NO_x$, and $SO_x$), which contribute to the increase of the greenhouse effect, leading to global warming and the increase of natural disasters, among others. For this reason, the use of biodiesel has been gaining more and more space in the world market. In addition to being a renewable fuel, it plays an excellent role for the environment, reducing emissions of harmful gases to the planet, compared to fossil fuels [1].

With the success of the global biodiesel industry, the production of glycerol also had a high growth rate. For each liter of biodiesel produced, 100 mL of crude glycerol, i.e., 10%, is obtained (**Figure 1**). Even if several industrialized products use glycerol in their formulation, the amount used in these products is not yet sufficient to meet the large production [2, 3].

The development of new technologies for the processing of the high availability of glycerol has been reported in the literature as one of the most promising goals of the present day regarding the transformation of glycerol into higher added value products. In turn, in industrial processes, this transformation of glycerol into higher added value products, such as solketal, is called glycerochemistry (**Figure 2**). The

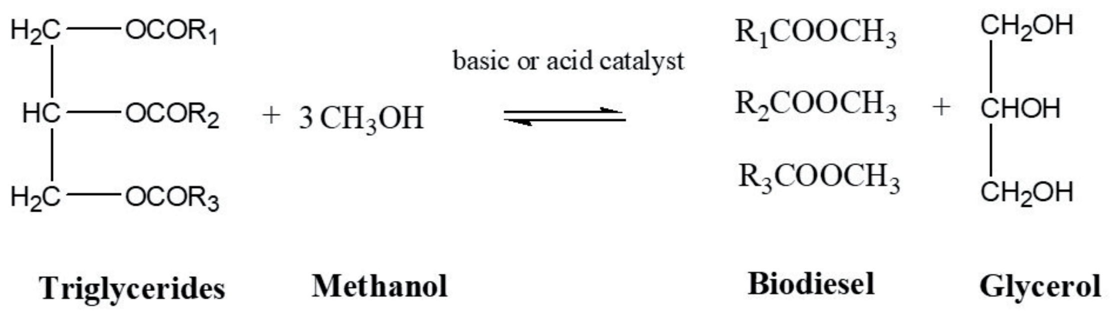

**Figure 1.**
*Reaction of biodiesel formation by triglyceride transesterification.*

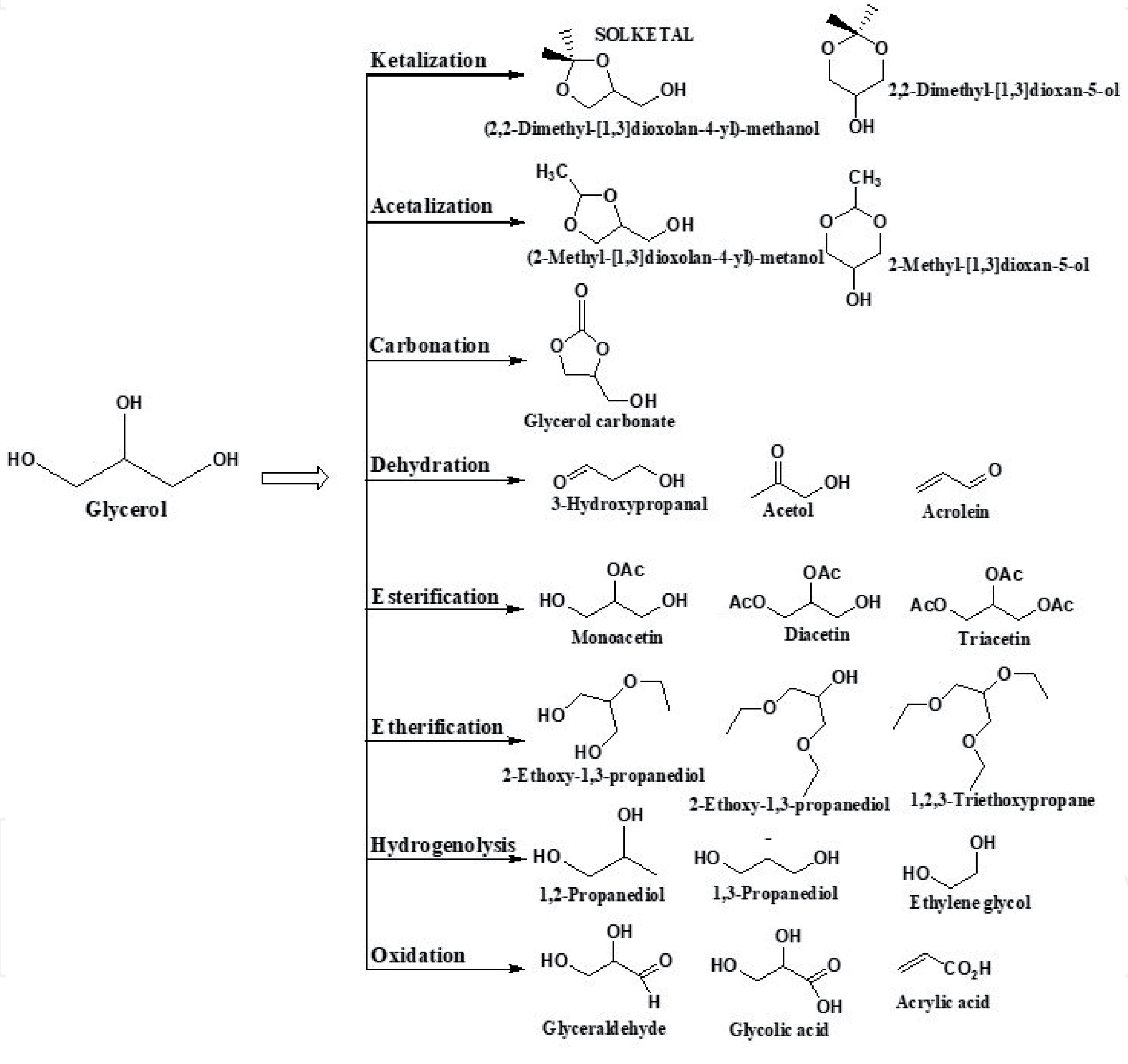

**Figure 2.**
*Transformation routes of glycerol into higher added value products.*

conversion of glycerol into other products can be accomplished by ketalization reactions, acetalization, carbonation, dehydration, esterification, etherification, hydrogenolysis, oxidation, and others [4].

In this work the focus is on the transformation of glycerol into solketal (isopropylidene glycerol or 2,2-dimethyl-1,3-dioxolan-4-yl methanol) (green solvent) through the ketalization reaction of glycerol with acetone. The reaction for solketal production is facilitated by major homogeneous and heterogeneous acid catalysts (**Figure 3**). The ketalization of glycerol with ketones generates branched oxygenates, solketal (2,2-dimethyl-[1,3] dioxan-4-yl methanol), and 2,2-dimethyl-[1,3]

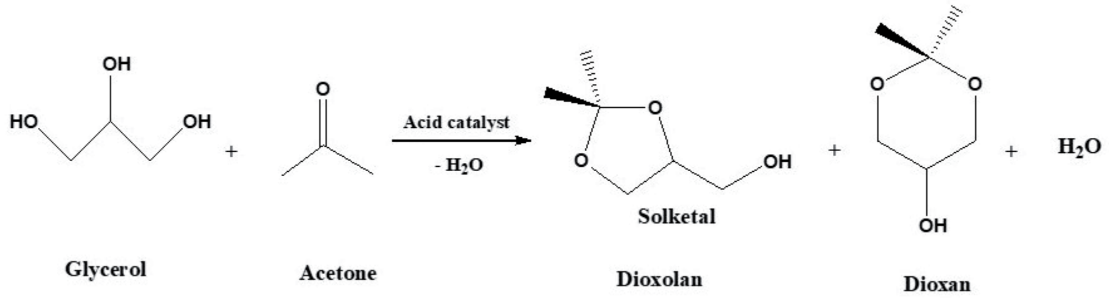

**Figure 3.**
*Solketal route production by ketalization of glycerol with acetone.*

dioxane-5-ol; however, when the reaction is carried out with acetone, the selectivity is higher for the solketal molecule, which has a five-membered ring [5].

Solketal is an excellent component for the formulation of gasoline, diesel, and biodiesel. The mixture of this compound in biofuels improves its properties, decreases viscosity, and helps to achieve the preestablished requirements for the flash point and oxidation stability of biodiesel. In addition, glycerol ketals are used as solvents, plasticizers, surfactants, disinfectants, and flavoring agents, among others. They can be used both in the pharmaceutical industry and in the food industry [5–7].

The commercial solketal is known as Augeo™ SL 191 and is produced by Rhodia (a member of the Solvay Group) and stands out as a slow evaporation solvent derived from glycerol which is considered a renewable source. Low toxicity to human health and the environment. It is a good solvent for resins and polymers, replacing solvents derived from petroleum and can be used as a (bio) fuel additive.

The synthesis of the solketal is catalyzed by p-toluenesulfonic acid (PTSA), Brönsted's acid used in homogeneous catalysis for 12 h at 100°C [8].

However, homogeneous Brönsted acid-type catalysts (hydrochloric, sulfuric, and p-toluenesulfonic acids, among others) have several disadvantages which reduce their usefulness, such as the difficulty of separation, inability to reuse, and corrosion of the reactor. The Menezes group (2013) proposed the use of homogeneous Lewis acid-type catalysts ($SnCl_2$, $SnF_2$, $Sn(OAc)_2$) that are easily recovered. The results showed that $SnCl_2$ was the most efficient and selective catalyst for solketal synthesis at room temperature. In addition to being easily recovered in the process of distillation of the reaction mixture, the catalyst can be reused for up to six times. The catalysts $SnF_2$ and $Sn\ (OAc)_2$ were not totally homogenized in the reaction mixture and therefore discarded. The use of $SnCl_2$ as a catalyst gave better and more economical results (at 25°C) than the conventional process, which uses PTSA as a catalyst [9].

Ferreira studied the reaction using a heteropolyacid based on phosphorus and tungsten immobilized on silica (PW-S), obtaining conversion and selectivity of 94 and 97%, respectively [10]. Silva and his group carried out tests using β-zeolite and Amberlyst™-15 polymer resin, resulting in conversions and selectivities of 90–95% and 90–95%, respectively [11]. Researchers Li et al. performed tests using MCM-41 mesoporous solid impregnated with tin (Sn-MCM-41) and USY zeolite, as catalysts, achieving conversions of 42 and 36%, respectively [12].

Khayoon [13] used activated mesoporous charcoal (AC) as a catalyst in the ketalization reaction of glycerol with acetone. The AC was impregnated with Ni and Zr, and the best result occurred when the carbon was impregnated with only 5% of metal and reached 98 and 86% selectivity, respectively. Using only active carbon as catalyst, they obtained 33% conversion and 81% selectivity. The results suggested that the improvement of these results was due to the addition of Lewis sites from nickel [13].

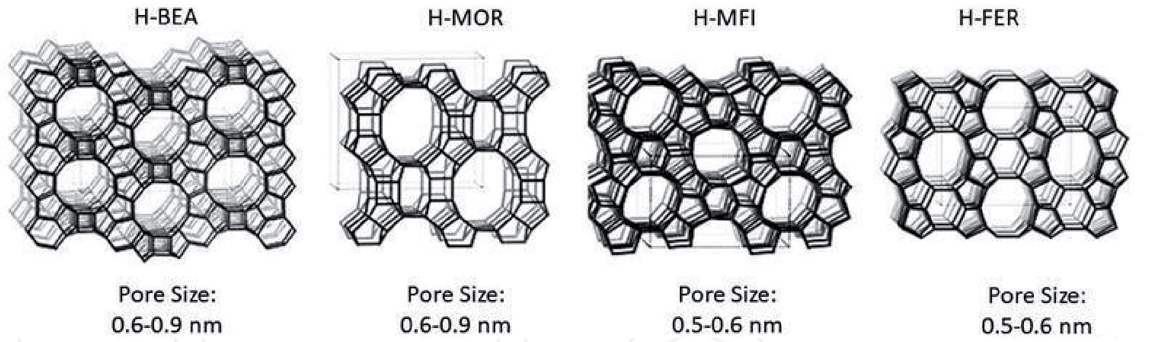

**Figure 4.**
*Structure and pore size of H-BEA, H-MOR, H-MFI, and H-FER zeolites.*

In this work, catalysts investigated for the transformation process of glycerol into solketal were acidic zeolites H-BEA, H-MOR, H-MFI, and H-FER (**Figure 4**) that can be easily recovered and reused in order to find new technological alternatives to improve the transformation routes of glycerol, a coproduct of the biodiesel industry, into products with higher added value.

## 2. Experimental

### 2.1 Reactants

The glycerol (99.5%) and acetone (99.5%) were purchased by the Brazilian industry PROQUÍMIOS.

### 2.2 Catalysts and characterizations

In this work, they used mordenite (MOR), MFI (H-ZSM-5), BEA (beta), and ferrierite (FER) acid zeolites. The zeolites were acquired in ammoniacal form, and then they were calcined at 500°C/4 h using a heating ramp of 10°C/min. After this process, the solids acquired acidic characteristics, and it is possible to use them as catalysts (H-BEA, H-MOR, H-MFI, and H-FER) in the ketalization reaction of glycerol with acetone. The catalysts were previously stored at a temperature of 100°C until the moment of reaction.

The X-ray diffraction analysis was performed to confirm the crystalline structure of the zeolites H-BEA, H-MOR, H-MFI, and H-FER before and after the calcination. The materials were characterized by X-ray diffraction in a Bruker D2 Phaser apparatus using CuKα radiation ($\lambda = 1.54$ Å) with a Ni filter, 0.02° pitch, 0.6 mm convergent slit, 10 mA current, and voltage of 30 kV, using a Lynxeye detector.

X-ray fluorescence analysis was used to verify the chemical composition of the H-BEA, H-MOR, H-MFI, and H-FER zeolites, which made the SAR calculation (silica:alumina ratio) possible. The pastille preparation was performed using approximately 500 mg of the sample and analyzed on a Bruker XRF-S2 Ranger spectrometer.

The textural analysis was used to calculate the specific areas, volumes, and pore sizes of the H-BEA, H-MOR, H-MFI, and H-FER zeolites by the Tristar 3000 Surface Area and Porosimetry Analyzer (Micromeritics) equipment. The specific area was obtained using the BET method (Brunauer, Emmet, and Teller); the specific volume and pore diameter were obtained by the BJH method from the adsorption/desorption isotherms. The samples, after weighing, were subjected to a drying heat treatment at 300°C under a vacuum of $5 \times 10^{-3}$ torr for a period of 24 h, then cooled to room temperature, and again weighed to start the analysis at a temperature of −196°C, thus obtaining the sorption (adsorption/desorption) isotherms of $N_2$ at different partial pressures of $N_2$.

The SEM analysis was performed on a Hitachi Tabletop Microscope TM-3000 using a high-sensitivity semiconductor backscattered electron detector.

The analysis of thermoprogrammed ammonia desorption was performed to calculate the total acidic strength and to classify and to quantify the type of strength (strong/weak) of the acid sites of the zeolites. The measures TPD-$NH_3$ of ammonia were performed on a Micrometrics 2910 equipment. The procedure took place in various steps. Firstly, the catalysts are subjected to a heat treatment in order to remove impurities physically adsorbed at the acid sites of the catalyst; for this a heating rate of 10°C/min up to 550°C/30 min was used in the presence of helium gas. After, the sample was cooled to 180°C with a stream of $NH_3$ (33 mL/min) for 30 min. Then, a helium flow was passed for 90 min in order to eliminate all the ammonia adsorbed physically in the catalyst. The analysis was terminated with the thermoprogrammed desorption of the ammonia which was chemically adsorbed at the acid sites of the catalyst; at this stage a heating rate of 15°C/min was used under the helium flow (30 mL/min) at temperature range between 180 and 550°C, after remaining for 30 min at 550°C. The ammonia desorbed at different temperatures was dragged by the current of helium gas that passed through a mass spectrometer (MS), thus making it possible to calculate TPD-$NH_3$ values of the acidity sites.

### 2.3 Catalytic tests

The catalytic tests for the ketalization reaction of glycerol with acetone were conducted in a batch reactor (V = 300 mL) which was fed with 40 g of glycerol (0.43 mol), 500 rpm, 60°C, and 5% of catalyst (in relation to mass of the limiting reactant), and molar ratio glycerol:acetone was 1:4. The conversion of the glycerol and the solketal selectivity were studied. The reaction time was 180 min, and aliquots were collected to monitor reaction kinetics. All reactions of this work were performed in triplicate. The reactor has thermocouple, transducer, temperature controller external heating mantle, and agitation system. At the end of the reactions, each reaction aliquot or suspension was filtered to separate the reaction/catalyst mixture. For the partial removal of water, 2 g of anhydrous sodium sulfate was added to the obtained mixture which was again filtered. All samples were stored at 15°C until analysis by GC-FID.

### 2.4 Reuse tests

Reused reactions of the catalysts and product analysis were carried out under the same conditions as the kinetic study with a reaction time of 60 min. Each catalyst (H-BEA, H-MOR, H-MFI, and H-FER) was used in five consecutive reactions. The product was filtered, and the catalyst returned to the reactor for the next reaction without pretreatments or washes, and so on.

### 2.5 Product analysis

The products of the glycerol ketalization reaction were analyzed quantitatively by means of a Shimadzu gas chromatograph with a flame ionization detector (CG-FID), using internal standardization methodology. The column employed was Carbowax (30 × 0.25 × 0.25 μm polyethylene glycol).

The internal calibration method was applied to glycerol (99.5%) and solketal (98%) chromatographic standards using 1,4-dioxane (99.8%) as the internal standard. Moreover, a response factor was introduced to correct the GC area and obtain quantitative results.

Calculations of conversion of glycerol ($X_{Gly}$) and selectivity to solketal ($S_{Skt}$), in percentage, were obtained by the following equations:

- Conversion of glycerol ($X_{Gly\%}$):

$$X_{Gly\%} = \frac{C_{Gly_0} - C_{Gly}}{C_{Gly_0}} 100 \tag{1}$$

where $C_{Gly0}$ is the molar concentration (mol/L) of glycerol at the beginning of the reaction and $C_{Gly}$ is the molar concentration (mol/L) of glycerol at the end of the reaction.

- Selectivity ($S_{Skt\%}$):

$$S_{Skt\%} = \frac{A_{Skt}}{A_{\mathrm{Products}}} 100 \tag{2}$$

where $A_{Skt}$ is the area of the desired product and $A_{Products}$ is the sum of the area of the solketal with the area of the unwanted products, obtained in the chromatograms.

## 2.6 Solketal characterization

At the end of the kinetic and/or catalytic tests in the GreenTec laboratory for the ketalization reaction of glycerol with acetone, the suspension remaining in the reactor composed of the glycerol-acetone/solketal-water/zeolites mixture H-BEA, H-MOR, H-MFI, and H-FER was filtered, and the liquid phase (reaction mixture) was stored in amber glass bottle. This reaction mixture was processed by rotoevaporation and fractional distillation. First, the reaction mixture was rotoevaporated to remove the remaining acetone. After the pH was adjusted between 5.5 and 6.5 with the addition of NaOH solution, 1 mol/L, to avoid the formation of other gases during the distillation process, store in a round-bottom flask containing pearls of glass, from the fractional distillation equipment (**Figure 5a**). The distillation was carried out in the Laboratory of Reactivity of Hydrocarbons, Biomass and Catalysis (LARHCO/UFRJ). Subsequently, the fractional distillation of the reaction mixture was performed (**Figure 5b**); the entire distillation process lasted for 4 h. After the distillation process, the fraction corresponding to Solketal was stored at 15°C, analyzed by FTIR, density, viscosity and water content for comparison with the analyzes of the commercial standard by the same analyzes.

The infrared spectra were obtained in a Fourier-transform infrared spectrophotometer, Nicolet model Magna-IR 760. Samples were analyzed on KBr pellets (400–4000 $cm^{-1}$). Number of scans: 16. Resolution: 4 $cm^{-1}$. The analyses were carried out in the Laboratory of Analyses of the Department of Inorganic Chemistry of IQ/UFRJ.

The specific density or mass of a sample is the ratio of the mass of a sample amount to the corresponding volume. This was determined by the Anton Paar Digital Density Meter, Model DMA 5000. The methodology for the analysis was performed according to ASTM D 4052.

Kinematic viscosity measures the flow time of a given volume of liquid flowing under the action of gravity by using a calibrated glass capillary viscometer. The method for determining this parameter was that presented in ASTM D 445.

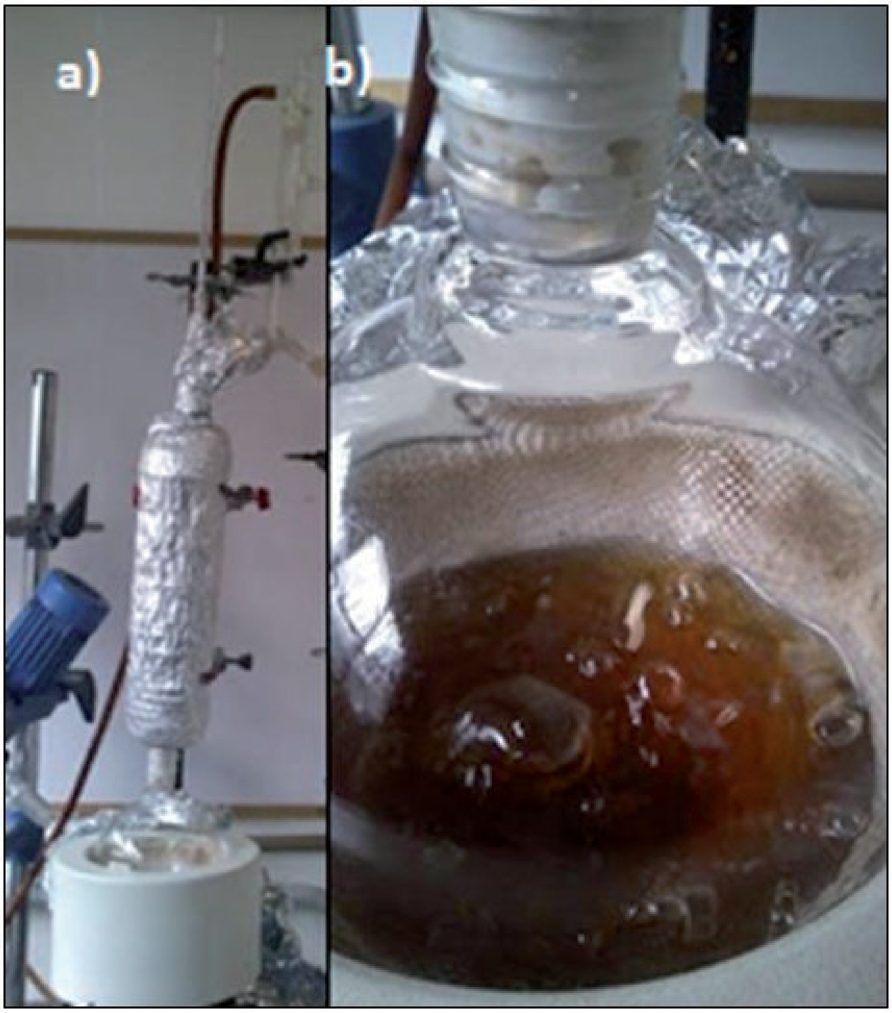

**Figure 5.**
*(a) Fractional distillation equipment and (b) reaction mixture to be distilled.*

For the water or moisture content test, the Karl Fischer coulometric method was used according to ASTM D 6304. The equipment used was the Karl Fischer METROHM titrator (model 756 KF) with the help of the Mettler XP-205 analytical balance.

## 3. Results and discussions

### 3.1 Catalysts characterization

**Figure 6** shows the X-ray diffractograms of the zeolites employed. When comparing them with those of literature [14, 15], the structure of the starting zeolites is confirmed, and that they have high crystallinity. The H-BEA, H-MOR, H-MFI, AND H-FER zeolite showed diffractograms similar to the standards of the International Zeolite Association (IZA) (www.iza-structure.org) [16].

The chemical composition of the zeolites was also studied by FRX, and the results are given in terms of oxides. The zeolites H-BEA, H-MOR, H-MFI, and H-FER are formed by oxides of silica and aluminum and also have small amounts of impurities. Through FRX analysis, it was also possible to determine the SARs ($SiO_2$/$Al_2O_3$ ratio) for each sample (**Table 1**).

Through SAR results, it is possible to have a slight notion about the Brönsted acidity of the zeolites used in this work, that is, the smaller the ratio, the greater the amount of aluminum in the structure and the greater the amount of compensation

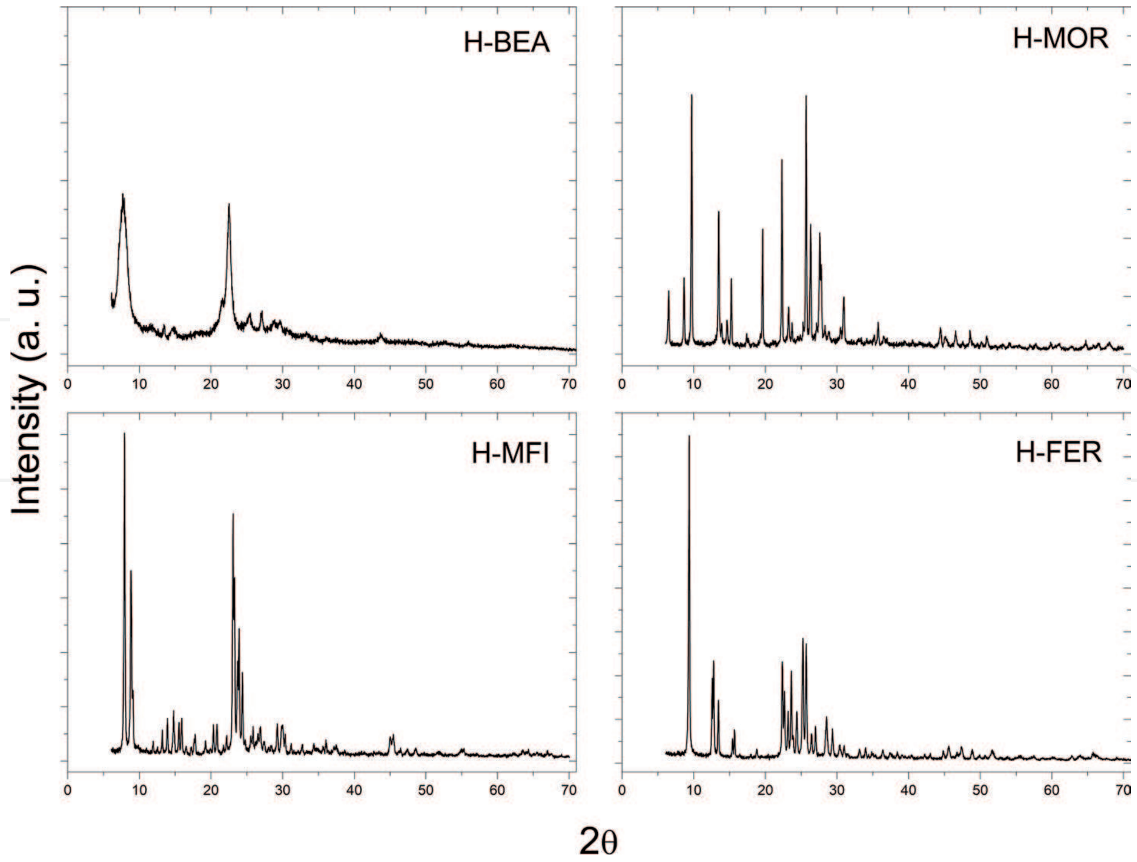

**Figure 6.**
*Diffractograms of zeolites H-BEA, H-MOR, H-MFI, and H-FER.*

| **Composition (%)** | **Catalysts** | | | |
|---|---|---|---|---|
| | **H-BEA** | **H-MOR** | **H-MFI** | **H-FER** |
| $SiO_2$ | 93.18 | 86.37 | 90.42 | 89.94 |
| $Al_2O_3$ | 5.58 | 12.38 | 7.11 | 9.15 |
| MgO | 0.50 | 0.60 | 0.50 | 0.50 |
| $Na_2O$ | 0.30 | 0.20 | 0.70 | — |
| Cl | 0.13 | 0.16 | 0.52 | 0.13 |
| $SO_3$ | 0.11 | 0.13 | 0.22 | 0.16 |
| $Fe_2O_3$ | 0.08 | 0.08 | 0.18 | 0.08 |
| $P_2O_5$ | 0.08 | — | — | — |
| $ZrO_2$ | 0.04 | — | — | — |
| $TiO_2$ | — | 0.02 | 0.21 | 0.04 |
| $ZrO_2$ | — | 0.03 | 0.05 | — |
| ZnO | — | 0.03 | — | — |
| $K_2O$ | — | — | 0.09 | — |
| SARs | 28 | 12 | 21 | 17 |

**Table 1.**
*Chemical composition and SARs of H-BEA, H-MOR, H-MFI, and H-FER zeolites by X-ray fluorescence.*

cations, providing a greater number of acidic sites in the zeolite [16, 17]. This acidity can be better studied by the analyses of TPD-NH3.

Scanning electron micrographs of the materials are shown in **Figure 7**, all on the same scale.

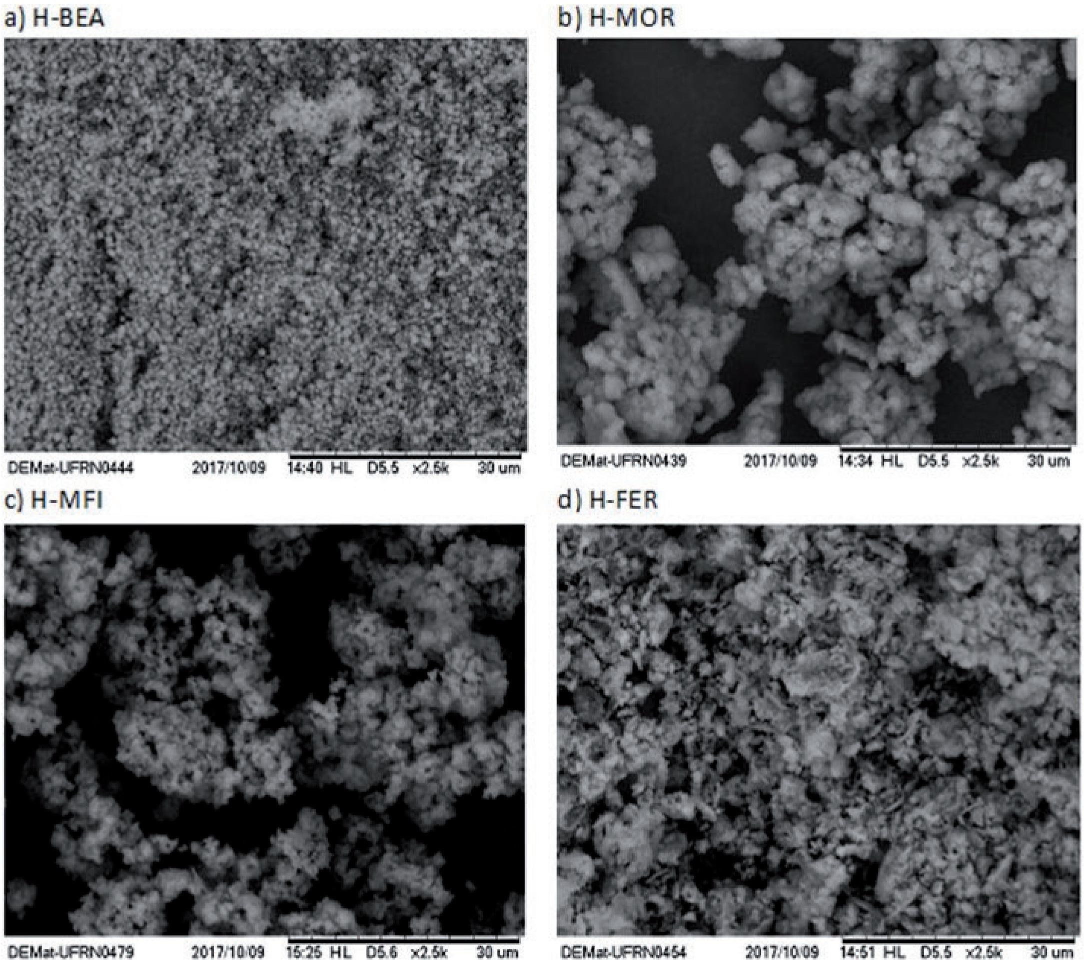

**Figure 7.**
*Micrographs of H-BEA (a), H-MOR (b), H-MFI (c), and H-FER (d) zeolites by X-ray fluorescence.*

| **Characteristics** | **H-BEA** | **H-MOR** | **H-MFI** | **H-FER** |
|---|---|---|---|---|
| Area$_{\text{BET}}$ [m$^2$/g] | 589 | 406 | 325 | 324 |
| Area$_{\text{MICROPOROS}}$ [m$^2$/g] | 439 | 367 | 229 | 291 |
| Area$_{\text{EXTERNAL}}$ [m$^2$/g] | 133 | 39 | 88 | 32 |
| Volume$_{\text{TOTAL}}$ [cm$^3$/g] | 0.30 | 0.21 | 0.14 | 0.17 |
| Volume$_{\text{MICROPOROS}}$ [cm$^3$/g] | 0.20 | 0.17 | 0.10 | 0.14 |
| Volume$_{\text{BJH/DES}}$ [cm$^3$/g] | 0.05 | 0.03 | 0.04 | 0.03 |
| Pore size$_{\text{BET}}$ [nm] | 2 | 2 | 2 | 2 |
| Pore size$_{\text{BJH/DES}}$ [nm] | 5 | 5 | 4 | 7 |

**Table 2.**
*Textural characteristics of H-BEA, H-MOR, H-MFI, and H-FER zeolites.*

It is observed that the H-BEA patches are smaller and appear to have a more homogeneous morphology. This is in agreement with the greater specific external area that this material has in relation to the others. The other materials have a more heterogeneous particle size distribution, and no definite shape is observed for the crystals. This may be due to the scale used in the micrograph or because they are commercial materials, which usually have a more heterogeneous morphology than those synthesized in the laboratory (on a lower-scale production).

By the adsorption analysis of $N_2$ (**Table 2**), it was observed that the materials are essentially microporous, characteristic of zeolitic materials. The H-BEA has the

| | Acidity (mmolNH$_3$/g$_{Cat}$) | | | |
|---|---|---|---|---|
| **Catalyst** | **Weak sites** | **Strong sites** | **Total acidity** | **F/f*** |
| H-BEA | 1.42 | 2.34 | 3.76 | 1.65 |
| H-MOR | 1.67 | 2.32 | 3.93 | 1.42 |
| H-MFI | 1.51 | 2.10 | 3.61 | 1.39 |
| H-FER | 1.60 | 1.83 | 3.43 | 1.14 |

**Ratio strong site: weak site.*

**Table 3.**
*Quantification of weak, strong, and total acidity sites.*

higher specific area due to its higher contribution of micropores and external area (due to smaller particle sizes).

Ammonia is often used as a probe molecule in acidity analyses because it has small molecular size, is stable, and possesses strong basic strength. The NH$_3$ thermoprogrammed desorption results of the H-BEA, H-MOR, H-MFI, and H-FER zeolites are shown in **Table 3**.

The zeolite H-BEA had the superior acid strength (2.34 mmolNH$_3$/g$_{cat}$) and bigger ratio of the strong:weak sites (1.65) than the other zeolites since this characteristic contributes to a higher catalytic activity for this reaction.

## 3.2 Kinetics and catalytic tests

The kinetic study, using the H-BEA, H-MOR, H-MFI, and H-FER catalysts, was carried out under the conditions chosen from the catalytic tests: 60° C, 550 rpm, 5% catalyst, and molar ratio glycerol:acetone 1:4. In this step, the results of conversion to glycerol and selectivity to the solketal were followed (**Figures 8** and 9).

In analyzing **Figures 8** and **9**, it is noted that the H-BEA catalyst gave the higher glycerol conversion, reaching 85% at 180 min. However, the H-FER catalyst ends

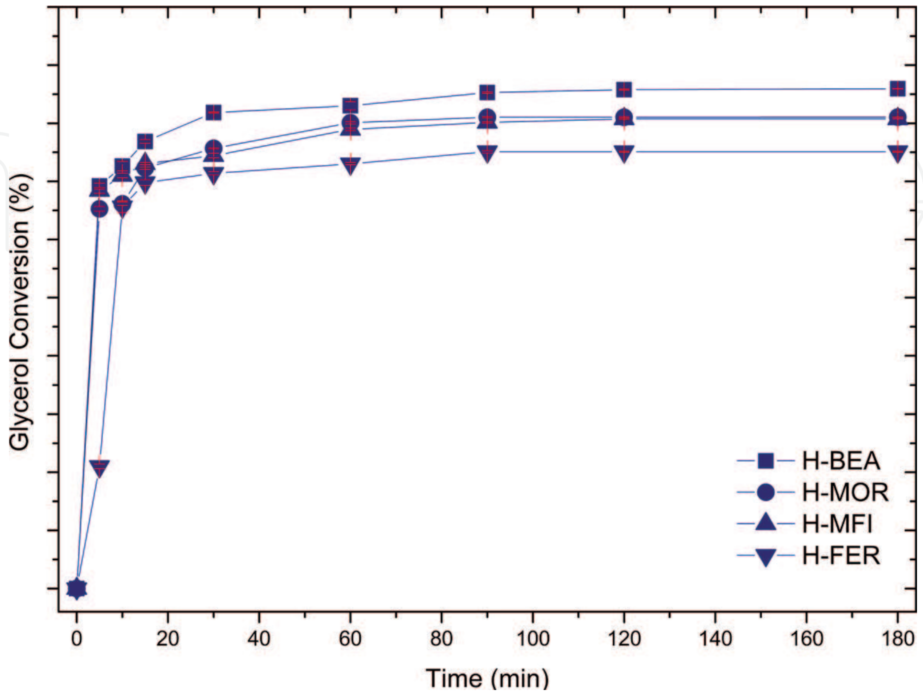

**Figure 8.**
*Glycerol conversion (%) using H-BEA, H-MOR, H-MFI, and H-FER zeolites as catalysts at 60° C, 550 rpm, 5% catalyst, and molar ratio glycerol:acetone 1:4.*

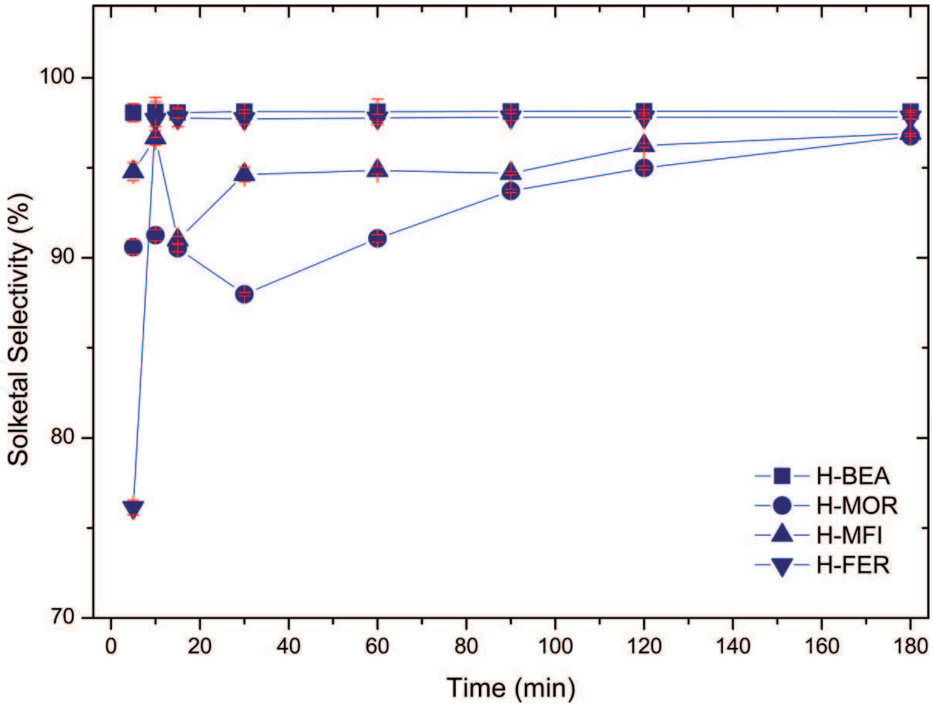

**Figure 9.**
*Solketal selectivity (%) using H-BEA, H-MOR, H-MFI, and H-FE zeolites as catalysts at 60° C, 550 rpm, 5% catalyst, and molar ratio glycerol:acetone 1:4.*

the reaction with 75% of glycerol conversion, while H-MOR and H-MFI had the same conversion, practically, at the end of the reaction, 180 min.

**Figure 8** shows that the most selective catalysts to solketal were H-BEA and H-MFI catalysts presenting values practically constant, on average 98 and 96%, respectively.

### 3.3 Catalytic activity

Many researchers have attempted to explain the activity and catalytic deactivation of the heterogeneous catalysts used in the ketalization reaction of glycerol with acetone using heterogeneous catalysts [17–25].

One factor that determines the activity of H-BEA zeolites is the size of the catalyst particle size and the presence of strong acid sites. The higher the SAR of the zeolite, the higher its acid strength and the lower the number of acid sites [17].

It is not only the acid sites of the catalyst that play an important role in the catalytic activity for this reaction but also the porosity of the catalyst [18]. Frisch (2003) concluded that the kinetic diameter of the reactants and the products of this reaction are in the range of 0.43–0.51 nm [19].

According to the literature, both Lewis acid and Brönsted acid sites are active for the ketalization reaction of glycerol with acetone [18–24].

Therefore, all the results obtained in this work can be based on the characteristics of the catalysts previously discussed in the literature. They can also help explain the data obtained in this work with zeolites H-BEA, H-MOR, H-MFI, and H-FER as catalysts. The characteristics of H-BEA contributed to it being the most active catalyst in the ketalization reaction of glycerol with acetone, when compared with the characteristics of H-FER. The zeolites H-MOR and H-MFI showed catalytic intermediate activity.

Even though acid catalysts have high activity, they can be deactivated by blocking the active sites by water molecules formed during the reaction. The higher the hydrophobicity of the catalyst, the lower the number of acid sites. However, hydrophobic groups act at the glycerol/acetone interface, reducing the interference of water molecules on the surface of the catalyst [20, 25].

Another approach, in terms of turnover frequency (TOF), the number of glycerol moles converted by moles of acidic site catalysts per hour, was performed at 60°C and 180 min, according to Eq. (3), [19]:

$$TOF = \frac{\left(\frac{NA_0 - NA}{N_{cat}}\right)}{t} \tag{3}$$

where $NA_0$ is amount of matter of glycerol at the initiation of the reaction, $NA$ is the amount of matter of glycerol in x time (x = 1, 2, and 3 h.), $N_{cat}$ is the amount of matter of the acidic site catalyst, and t is the time in hours (h). The *TOF* values at 1, 2, and 3 h are presented in **Figure 10**.

The value of TOF tends to decrease with the passage of time. This observation is explained by the loss of catalytic activity or by the reaction reaching an equilibrium for reversible reactions. TOF values were practically the same, 47 $h^{-1}$ for H-BEA, H-MFI, and H-FER catalysts. However, the H-MOR catalyst presented TOF a little inferior, 44 $h^{-1}$, when compared to the other catalysts, in all times of reaction. This means that from this perspective, all catalysts have basically the same activity.

### 3.4 Reuse testing

The reuse experiments were done for all catalysts under the same conditions used in the kinetic study. To perform these experiments, at the end of the reaction, the catalyst was only separated from the reaction solution by filtration and then reused four more times in the same manner. The reason why we chose to perform the reuse tests without the need for pretreatments (washing and calcination) for the catalysts between the reactions was to avoid the loss of time in the reuse tests and loss of material by manipulation. Because, industrially, it is not feasible to stop the

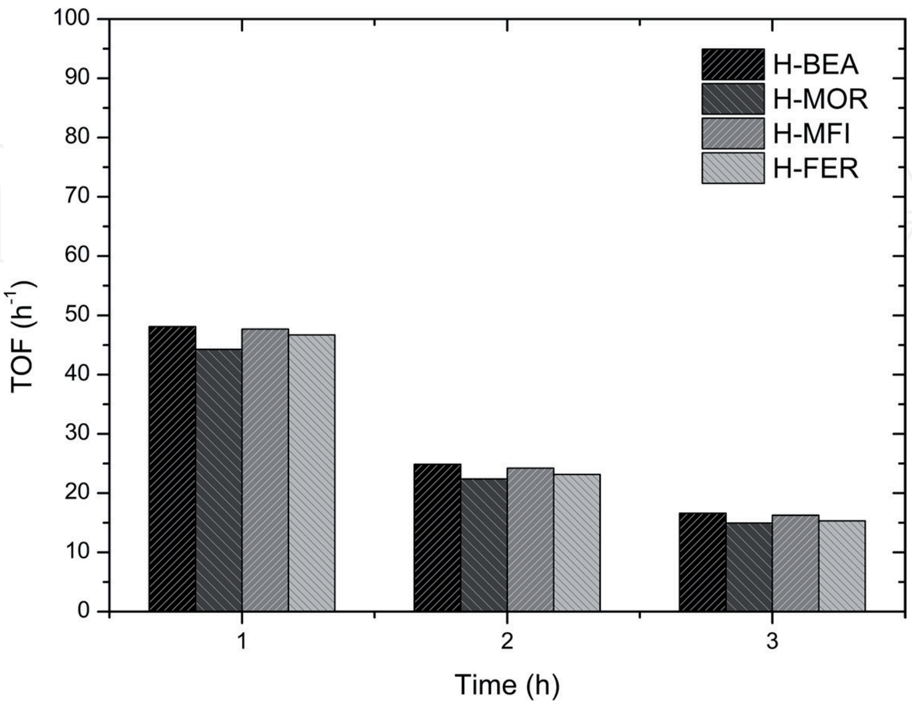

**Figure 10.**
*Results of catalytic activity by TOF using H-BEA, H-MOR, H-MFI, and H-FER zeolites as catalysts at 60°C, 550 rpm, 5% catalyst, and molar ratio glycerol:acetone 1:4, for 1, 2, and 3 h.*

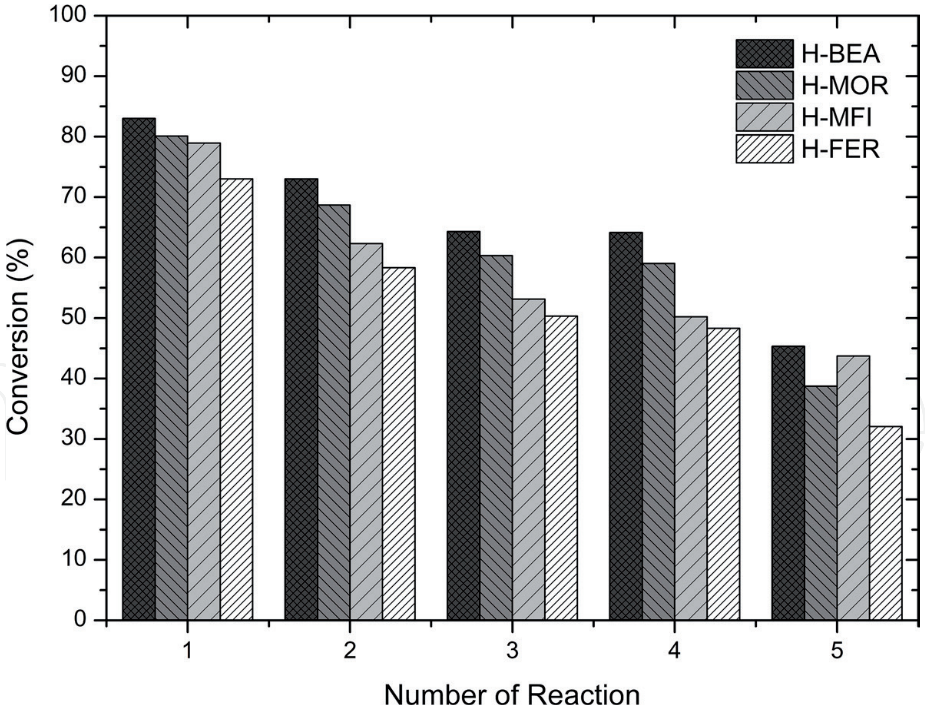

**Figure 11.**
*Solketal conversion (%) in reuse tests using H-BEA, H-MOR, H-MFI, and H-FER zeolites as catalysts at 60°C, 550 rpm, 5% catalyst, and molar ratio glycerol:acetone 1:4, 60 min.*

production to wash and calcine the catalyst every 60 min, the study was carried out in a batch reactor.

**Figure 11** shows the glycerol conversion results after each reuse experiment of the H-BEA, H-MOR, H-MFI, and H-FER catalysts.

According to **Figure 11**, the H-BEA catalyst in its first use shows an excellent conversion of glycerol to the ketalization reaction of glycerol with acetone, reaching 85% conversion of glycerol and selectivity 98%. In the fourth reuse, the conversion of glycerol reaches 55% on average. The solketal selectivity remains constant throughout the process ≈98%. For the H-MOR catalyst, the conversion of glycerol drops gradually, after each reuse, and varies between 80 and 35%, and solketal selectivity remains constant, 96%. For the H-MFI catalyst, the conversion of glycerol drops gradually, after each reuse, and varies between 80 and 45%, and selectivity to solketal varies between 95 and 90%. For the H-FER catalyst, the conversion of glycerol drops gradually, after each reuse, and varies between 75 and 30%. And its selectivity to solketal varies between 90 and 85%.

It is known that some of the water produced during the reaction and/or impurities of the reactants such as sodium residues in the glycerol together with the catalyst friction on the reactor walls have destabilized the structure of the H-BEA, H-MOR, H-MFI, and H-FER catalysts, altering their crystallinity and assisting in deactivation [4].

### 3.5 Product characterization

During the distillation process of the reaction products mixture, it was observed that when the distillation is carried out under vacuum between the temperatures 30 and 69°C, it occurs that the output of the remaining acetone and water between 70 and 120°C plus a fraction containing solketal is distilled. Glycerol is only removed when the system reaches 200°C. The yield of the distillation was 60% by mass of solketal over the initial blend (solketal-water-glycerol-traces of acetone). The solketal fraction is colorless but with a lower viscosity than glycerol.

**Figure 12.**
*Appearance of the GreenTec solketal fraction.*

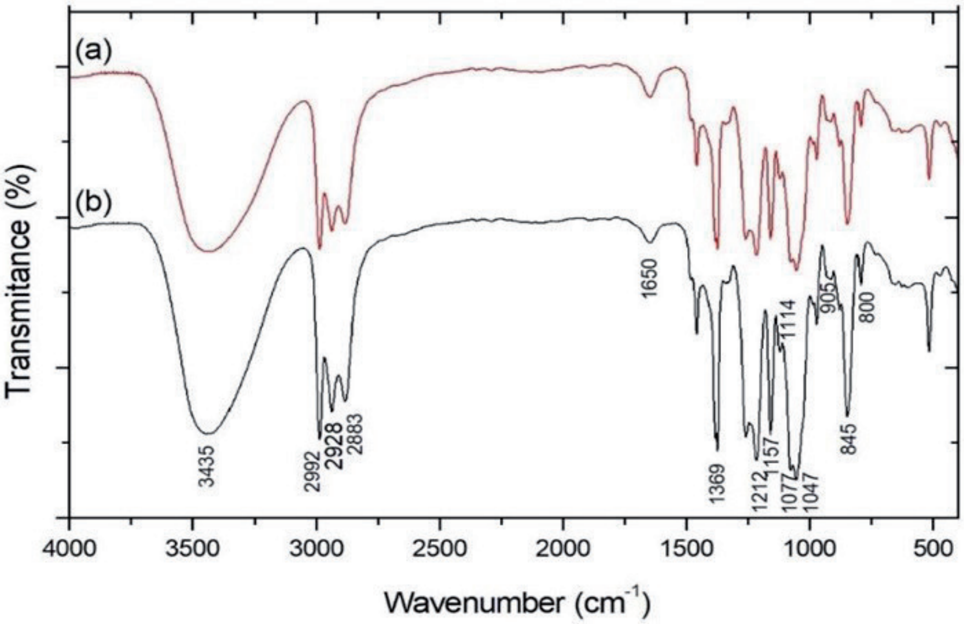

**Figure 13.**
*Infrared spectra of solketal GreenTec (a) and solketal sigma-Aldrich (b).*

**Figure 12** shows the appearance of the solketal GreenTec fraction after distillation of the initial blend.

FTIR analysis was used to confirm the presence of solketal in the distilled product and to compare it with its Sigma-Aldrich standard. The FTIR spectrum of the solketal GreenTec and solketal Sigma-Aldrich samples is shown in **Figure 13**.

**Figure 13** shows a strong band at 3435 $cm^{-1}$ which is attributed to the axial deformation of the —O —H bonds originating from the hydroxyls and hydrogen bonds between solketal molecules. The region comprising the wave numbers between 2992 and 2883 $cm^{-1}$ refers to the symmetrical axial deformation bands and asymmetric axial deformation of the —C —H bonds of the methyls.

| **Solketal** | **Density** | **Viscosity** |
|---|---|---|
| | **[g/cm$^3$] ± DP** | **[mm$^2$/s] ± DP** |
| Sigma-Aldrich | 1.0666 ± 0.0006 | 5.2030 ± 0.0008 |
| GreenTec | 1.0584 ± 0.0148 | 5.1650 ± 0.0123 |

**Table 4.**
*Results of density or specific gravity analysis and kinematic viscosity for solketal.*

| **Solketal** | **Water content** | | | |
|---|---|---|---|---|
| | **[ppm]** | **[%]** | **[g/L]** | **[mol/L]** |
| Sigma-Aldrich | 390 | 0.0390 | 0.3900 | 0.0217 |
| GreenTec | 610 | 0.0610 | 0.6100 | 0.0334 |

**Table 5.**
*Results of water content analysis for Solketal.*

The angular deformation of the water was attributed in the localized band appearing at 1650 cm$^{-1}$. The band located at 1369 cm$^{-1}$ refers to the movement of “umbrella” referring to the methyls of the ketone group. The bands observed at 1212 and 1077 cm$^{-1}$ refer to the —C —O bonds of the five-membered ring (dioxolanes), bands of greater importance.

The bands at 1157 and 1114 cm$^{-1}$ refer to the asymmetric vibrational motion of the —C —O —C —O —C — bonds of solketal. However, bands between 905 and 800 cm$^{-1}$ are attributed to the symmetrical vibrational movement of these same bonds. To finalize, the band located at 1047 cm$^{-1}$, the —C —C —OH bond of the alcoholic group 4 was assigned.

**Tables 4** and **5** present the results of density, viscosity, and water or moisture content for the solketal Sigma-Aldrich standard and the solketal produced by GreenTec.

When analyzing **Table 4**, it is observed that both solketal Sigma-Aldrich and solketal GreenTec present very close densities and viscosities.

**Table 5** shows that only in the analysis of humidity a significant difference between the solketal samples was noticed.

Solketal GreenTec presents 56.41% more humidity than solketal Sigma-Aldrich. To remove this moisture, anhydrous sodium sulfate may be added among other drying agents, and/or the solketal GreenTec fraction is withdrawn from 75°C.

## 4. Conclusions

Glycerol to solketal transformation is possible to carry out using zeolite acidic catalysts, such as H-BEA, H-MOR, H-MFI, and H-FER, showing a very good activity (conversion 85%) and selectivity (98%). H-BEA presented a larger area, major SAR, and a bigger ratio of the strong:weak sites than the other zeolites. This characteristic contributes to a higher catalytic activity for H-BEA catalyst. All the catalysts can be reused for four times without washing or pretreatment among reactions in batch reactor, but the best catalyst is still the H-BEA zeolite for being more active and showing constant solketal selectivity. The solketal produced in this work was characterized by comparing it with its commercial standard, obtaining very similar characteristics.

## Acknowledgements

The authors thank the following: CAPES, CNPq, TPQB/EQ/UFRJ, IQ/UFRJ, and William Xavier.

## Conflict of interest

There are no conflicts of interest in this publication.

## Appendices and nomenclature

| | |
|---|---|
| H-BEA | acid beta zeolite |
| H-MOR | acid mordenite zeolite |
| H-MFI | acid ZSM-5 zeolite |
| H-FER | acid ferrierite zeolite |
| TPD-NH3 | temperature-programmed desorption of ammonia |
| FTIR | Fourier-transform infrared spectroscopy |
| TOF | turnover frequency |

## Author details

Vinicius Rossa[1]*, Gisel Chenard Díaz[2], Germildo Juvenal Muchave[2],
Donato Alexandre Gomes Aranda[2] and Sibele Berenice Castellã Pergher[3]

1 Federal University of Uberlândia, Uberlândia, MG, Brazil

2 Federal University of Rio de Janeiro, Rio de Janeiro, RJ, Brazil

3 Federal University of Rio Grande do Norte, Natal, RN, Brazil

*Address all correspondence to: vinnyrossa@gmail.com

## References

[1] Pinto AG, Guarieiro LN, Resende MJC. Biodiesel: An overview. Journal of the Brazilian Chemical Society. 2005;**513**:1313-1330. DOI: 10.1590/S0103-50532005000800003

[2] Adhikari S, Fernando S, Haryanto A. Production of hydrogen by steam reforming of glycerin over alumina-supported metal catalysts. Catalysis Today. 2007;**129**:355-364. DOI: 10.1016/j.cattod.2006.09.038

[3] Sánchez EA, D'angelo MA, Comelli RA. Hydrogen production from glycerol on Ni/$Al_2O_4$ catalyst. International Journal of Hydrogen Energy. 2010;**35**:5902-5907. DOI: 10.1016/j.ijhydene.2009.12.115

[4] Rossa V. Catalytic systems for the conversion of glycerol to solketal—"Green Solvent" [thesis]. Rio de Janeiro: Federal University of Rio de Janeiro; 2017

[5] Royon D, Locatelli S, Gonzo EE. Ketalization of glycerol to solketal in supercritical acetone. Journal of Supercritical Fluids. 2011;**58**:88-92. DOI: 10.1016/j.supflu.2011.04.01

[6] Mota CJA, Silva CXX, Gonçalves VLC. Gliceroquímica: Novos produtos e processos a partir da glicerina de produção de biodiesel. Química Nova. 2009;**32**:639-648. Available from: http://www.scielo.br/pdf/qn/v32n3/a08v32n3.pdf

[7] Reddy PS, Sudarsanam P, Mallesham B, Raju G, Reddy BM. Acetalisation of glycerol with acetone over zirconia and promoted zirconia catalysts under mild reaction conditions. Journal of Industrial and Engineering Chemistry. 2011;**17**: 377-381. DOI: 10.1016/j.jiec.2011.05.008

[8] Suriyaprapadilok N, Kitiyanan B. Synthesis of solketal from glycerol and its reaction with benzyl alcohol. Energy Procedia. 2011;**9**:63-69. DOI: 10.1016/j.egypro.2011.09.008

[9] Menezes FDL, Guimaraes MDO, Silva MJD. Highly selective $SnCl_2$-catalyzed Solketal synthesis at room temperature. Industrial and Engineering Chemistry Research. 2013;**52**:16709-16713. DOI: 10.1021/ie402240j

[10] Ferreira P, Fonseca IM, Ramos AM, Vital J, Castanheiro JE. Valorisation of glycerol by condensation with acetone over silica-included heteropolyacids. Applied Catalysis B: Environmental. 2010;**98**:94-99. DOI: 10.1016/j.apcatb.2010.05.018

[11] Silva B, Figueiredo H, Santos VP, Pereira MFR, Figueiredo JL, Lewandowsk EA, et al. Reutilization of Cr-Y zeolite obtained by biosorption in the catalytic oxidation of volatile organic compounds. Journal of Hazardous Materials. 2011;**192**:545-553. DOI: 10.1016/j.jhazmat.2011.05.056

[12] Li L, Korányi TI, Sels BF, Pescarmona PP. Highly-efficient conversion of glycerol to solketal over heterogeneous Lewis acid catalysts. Green Chemistry. 2012;**14**:1611-1619. DOI: 10.1039/C2GC16619D

[13] Khayoon MS, Hameed BH. Solventless acetalization of glycerol with acetone to fuel oxygenates over Ni–Zr supported on mesoporous activated carbon catalyst. Applied Catalysis A: General. 2013;**464-465**:191-199. DOI: 10.1016/j.apcata.2013.05.035

[14] Mignoni ML, Detoni C, Pergher SBC. Estudo da síntese da zeólita ZSM-5 a partir de argilas naturais. Química Nova. 2007;**30**(1):45-48. DOI: 10.1590/S0100-40422007000100010

[15] Treacy MMJ, Higgins JB. Collection of Simulated XRD Powder Patterns for Zeolites. 5th ed. Amsterdan:

Elsevier; 2007. pp. 11-480. ISBN: 978-0-444-53067-7

[16] Sheemol VN, Tyagi B, Jasra RV. Acylation of toluene using rare earth cation exchanged zeolite β as solid acid catalyst. Journal of Molecular Catalysis A: Chemical. 2004;**215**:201-208. DOI: 10.1016/j.molcata.2004.02.002

[17] Braga A, Morgon NH. Descrições estruturais cristalinas de zeólitos. Química Nova. 2007;**30**:178-188. DOI: 10.1590/S0100-40422007000100030

[18] Gadamsetti S, Rajan NP, Rao GS, Chary KVR. Acetalization of glycerol with acetone to bio fuel additives over supported molybdenum phosphate catalysts. Journal of Molecular Catalysis A: Chemical. 2015;**410**:49-57. DOI: 10.1016/j.molcata.2015.09.006

[19] Rossa V, Pessanha Y d SP, Díaz GC, Câmara LDT, Pergher SBC, Aranda DAG. Reaction kinetic study of Solketal production from glycerol Ketalization with acetone. Industrial and Engineering Chemistry Research. 2017;**56**(2):479-488. DOI: 10.1021/acs.iecr.6b03581

[20] Sandesh S, Halgeri AB, Shanbhag GV. Utilization of renewable resources: Condensation of glycerol with acetone at room temperature catalyzed by organic-inorganic hybrid catalyst. Journal of Molecular Catalysis A: Chemical. 2015;**401**:73-80. DOI: 10.1016/j.molcata.2015.02.015

[21] Kowalska-kus J, Held A, Nowinska K. Enhancement of the catalytic activity of H-ZSM-5 zeolites for glycerol acetalization by mechanical grinding. Reaction Kinetics, Mechanisms and Catalysis. 2016;**117**:341-352. DOI: 10.1007/s11144-015-0922-4

[22] Nanda MR, Zhang Y, Yuan Z, Qin W, Ghaziaskar HS, Xu CC. Catalytic conversion of glycerol for sustainable production of solketal as a fuel additive: A review. Renewable and Sustainable Energy Reviews. 2016;**56**:1022-1031. DOI: 10.1016/j.rser.2015.12.008

[23] Stawicka K, Díaz-álvarez AE, Calvino-casilda V, Trejda M, Bañares MA, Ziolek M. The role of Brønsted and Lewis acid sites in acetalization of glycerol over modified mesoporous cellular foams. Journal of Physical Chemistry C. 2016;**120**:16699-16711. DOI: 10.1021/acs.jpcc.6b04229

[24] Venkatesha NJ, Bhat YS, Jai Prakash BS. Dealuminated BEA zeolite for selective synthesis of five-membered cyclic acetal from glycerol under ambient conditions. RSC Advances. 2016;**6**:18824-18833. DOI: 10.1039/C6RA01437B

[25] Silva CXAD, Mota CJA. The influence of impurities on the acid-catalyzed reaction of glycerol with acetone. Biomass and Bioenergy. 2011;**35**:3547-3551. DOI: 10.1021/ef9015735